

OXYGEN-RICH MASS LOSS WITH A PINCH OF SALT: NaCl IN THE CIRCUMSTELLAR GAS OF IK TAURI AND VY CANIS MAJORIS

S. N. MILAM, A. J. APPONI, N. J. WOOLF, AND L. M. ZIURYS

Department of Chemistry, Department of Astronomy, NASA Astrobiology Institute, and Steward Observatory, University of Arizona,
933 North Cherry Avenue, Tucson, AZ 85721; stemil@as.arizona.edu, aapponi@as.arizona.edu,
nwoolf@as.arizona.edu, lziurys@as.arizona.edu

Received 2007 June 30; accepted 2007 August 31; published 2007 October 4

ABSTRACT

The NaCl molecule has been observed in the circumstellar envelopes of VY Canis Majoris (VY CMA) and IK Tauri (IK Tau)—the first identifications of a metal refractory in oxygen-rich shells of evolved stars. Five rotational transitions of NaCl at 1 and 2 mm were detected toward VY CMA and three 1 mm lines were observed toward IK Tau, using the telescopes of the Arizona Radio Observatory. In both objects, the line widths of the NaCl profiles were extremely narrow relative to those of other molecules, indicating that sodium chloride has not reached the terminal outflow velocity in either star, likely a result of early condensation onto grains. Modeling the observed spectra suggests abundances, relative to H₂, of $f \sim 5 \times 10^{-9}$ in VY CMA and $f \sim 4 \times 10^{-9}$ in IK Tau, with source sizes of 0.5'' and 0.3'', respectively. The extent of these sources is consistent with the size of the dust acceleration zones in both stars. NaCl therefore appears to be at least as abundant in O-rich shells as compared to C-rich envelopes, where $f \sim (0.2\text{--}2) \times 10^{-9}$, although it appears to condense out earlier in the O-rich case. Chemical equilibrium calculations indicate that NaCl is the major carrier of sodium at $T \sim 1100$ K for oxygen-rich stars, with predicted fractional abundances in good agreement with the observations. These measurements suggest that crystalline salt may be an important condensate for sodium in both C- and O-rich circumstellar shells.

Subject headings: astrochemistry — radio lines: stars — stars: chemically peculiar — stars: individual (VY Canis Majoris, IK Tauri, IRC +10216)

1. INTRODUCTION

Molecular material has been known for decades to exist in the envelopes of both carbon- and oxygen-rich evolved stars, primarily in the form of CO, SiO, and HCN. However, chemical complexity has been usually associated with C-rich asymptotic giant branch (AGB) stars and their successors, protoplanetary nebulae (Pardo et al. 2007). For example, in the shell of the AGB star IRC +10216, where C > O, over 60 molecular species have been detected, including sodium-, magnesium-, and aluminum-bearing compounds, as well as silicon and carbon chain compounds (Cernicharo & Guélin 1987; Turner et al. 1994; Kawaguchi et al. 1993; Ziurys et al. 1994, 1995, 2002).

Some of the exotic types of species found in carbon-rich envelopes are those containing sodium. In IRC +10216, for example, two sodium-bearing molecules have been detected: NaCl and NaCN (Cernicharo & Guélin 1987; Turner et al. 1994). These species have been found to have a confined, inner-envelope distribution in this object, with a source size of $\theta_s \sim 5''$, corresponding to a radius of ~ 86 stellar radii, or $86R_*$ (Guélin et al. 1996). More recently, NaCl and NaCN have been detected in CRL 2688 as well. These sodium-containing species are thought to be produced by equilibrium chemistry near the stellar photosphere (Tsuji 1973), although additional chemical effects exist in CRL 2688 because the object is undergoing a second, enhanced phase of mass loss (Highberger & Ziurys 2003; Highberger et al. 2003).

Here we present the first detections of NaCl in oxygen-rich circumstellar envelopes. Sodium chloride has been observed in the supergiant star VY Canis Majoris (VY CMA) and the Mira variable IK Tauri (IK Tau). This species has been identified via measurements of multiple rotational transitions at $\lambda = 1$ and 2 mm using the Arizona Radio Observatory (ARO). The spectra suggest a strictly inner-envelope distribution, within $50R_*$. The original detection of NaCl toward VY CMA

was mentioned in a previous publication (Ziurys et al. 2007). In this Letter we present the results for NaCl in detail and discuss their implications for circumstellar sodium chemistry.

2. OBSERVATIONS

Observations at 1 mm were conducted at the ARO with the Submillimeter Telescope (SMT) on Mount Graham, Arizona, and measurements at 2 mm with the 12 m telescope at Kitt Peak, Arizona, during the period from 2006 February to 2007 March. The receiver at the SMT was an image-separating Atacama Large Millimeter Array (ALMA) Band 6 mixer; the lower sideband was used for the measurements (Lauria et al. 2006). Rejection for the image, in this case, upper sideband, was typically >20 dB. The back end employed was a 2048 channel, 1 MHz filter bank. At the 12 m, a dual-channel SIS receiver was used, operated in single sideband mode with image rejection >18 dB. Spectrometer back ends utilized at this facility were 1 and 2 MHz resolution filter banks, configured in parallel mode for the two receiver channels. The temperature scale at the SMT is T_A^* and at the 12 m, T_R^* . Conversion to radiation temperature is then $T_R = T_A^*/\eta_B$ and $T_R = T_R^*/\eta_c$, where η_B is the main-beam efficiency and η_c is the beam efficiency corrected for forward spillover losses. Observations were conducted in beam-switching mode with a subreflector throw of $\pm 2'$ toward VY CMA (B1950.0: $\alpha = 07^{\text{h}}20^{\text{m}}54.7^{\text{s}}$, $\delta = -25^{\circ}40'12''$) and IK Tau (B1950.0: $\alpha = 03^{\text{h}}50^{\text{m}}43.6^{\text{s}}$, $\delta = 11^{\circ}15'32''$). Supporting measurements were additionally carried out toward IRC +10216 (B1950.0: $\alpha = 09^{\text{h}}45^{\text{m}}14.8^{\text{s}}$, $\delta = 13^{\circ}30'40''$) at 1 and 2 mm. Pointing and focus corrections were established by frequent observations of planets. Frequencies and telescope parameters are given in Table 1.

TABLE 1
OBSERVATIONS OF NaCl TOWARD VY CMa, IK TAU, AND IRC +10216

Source	Transition	Frequency (MHz)	θ_b (arcsec)	η_c or η_b	T_A^* (K)	V_{LSR} (km s $^{-1}$)	$\Delta V_{1/2}$ (km s $^{-1}$)
VY CMa ^a	$J = 11 \rightarrow 10$	143237.37	44	0.76	0.003 ± 0.001^d	18.0 ± 2.1	18.8 ± 2.1
	$J = 17 \rightarrow 16$	221260.11	34	0.78	0.008 ± 0.004	17.7 ± 2.7	15.0 ± 2.7
	$J = 18 \rightarrow 17$	234251.87	32	0.78	0.013 ± 0.005	17.4 ± 2.6	14.1 ± 2.6
	$J = 19 \rightarrow 18$	247239.59	30	0.78	0.014 ± 0.005	16.7 ± 2.4	14.5 ± 2.4
	$J = 20 \rightarrow 19$	260223.06	29	0.78	0.014 ± 0.010	16.0 ± 3.5	18.4 ± 3.5
IK Tau ^b	$J = 18 \rightarrow 17$	234251.87	32	0.78	0.005 ± 0.004	28.0 ± 2.6	6.4 ± 2.6
	$J = 19 \rightarrow 18$	247239.59	30	0.78	0.006 ± 0.004	27.9 ± 2.4	4.2 ± 2.4
	$J = 20 \rightarrow 19$	260223.06	29	0.78	0.006 ± 0.003	29.5 ± 2.4	5.7 ± 2.4
IRC +10216 ^c	$J = 10 \rightarrow 9$	130223.68	48	0.80	0.026 ± 0.006	-27.7 ± 4.6	19.1 ± 4.6
	$J = 17 \rightarrow 16$	221260.11	34	0.78	0.023 ± 0.008	-26.1 ± 2.8	19.6 ± 2.8
	$J = 18 \rightarrow 17$	234251.87	32	0.78	0.028 ± 0.013	-27.6 ± 2.6	21.6 ± 2.6
	$J = 19 \rightarrow 18$	247239.59	30	0.78	0.026 ± 0.008	-26.3 ± 2.4	19.1 ± 2.4
	$J = 20 \rightarrow 19$	260223.06	29	0.78	0.062 ± 0.034	-26.7 ± 2.3	19.0 ± 2.3

^a $\alpha = 07^{\text{h}}20^{\text{m}}54.7^{\text{s}}$, $\delta = -25^{\circ}40'12''$ (B1950.0).

^b $\alpha = 03^{\text{h}}50^{\text{m}}43.6^{\text{s}}$, $\delta = 11^{\circ}15'32''$ (B1950.0).

^c $\alpha = 09^{\text{h}}45^{\text{m}}14.8^{\text{s}}$, $\delta = 13^{\circ}30'40''$ (B1950.0).

^d Intensity scale was corrected from T_R^* to T_A^* ; $\eta_{\text{iss}} = 0.68$.

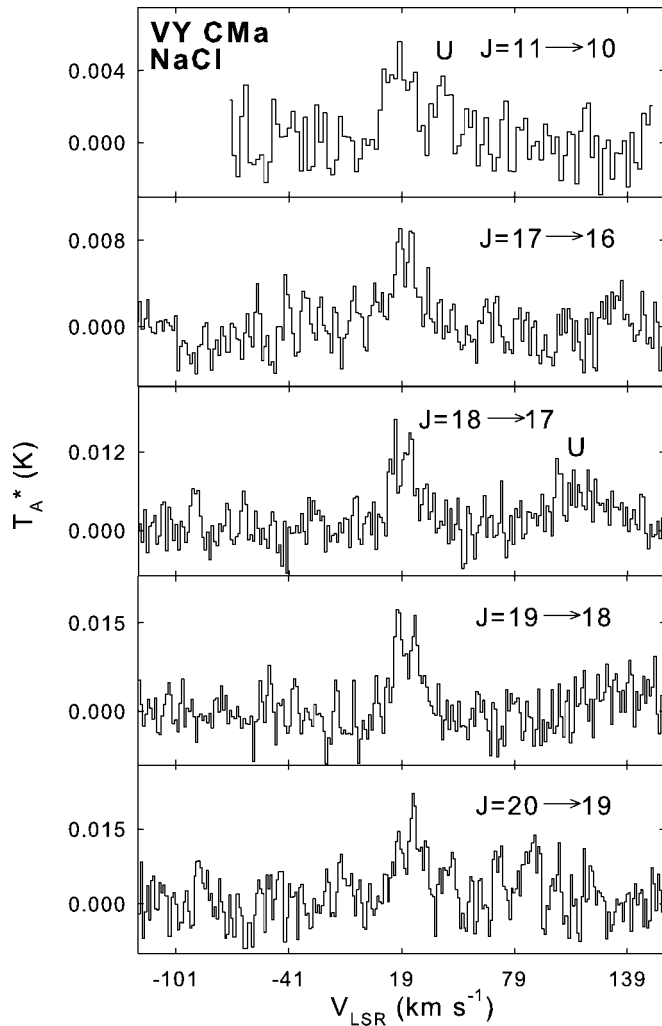


FIG. 1.—Spectra of the five rotational transitions of NaCl observed toward VY CMa using the ARO 12 m and SMT telescopes at 143, 221, 234, 247, and 260 GHz, respectively. Spectral resolution is 1 MHz, and the temperature scale is T_A^* . (The 12 m data, $J = 11 \rightarrow 10$, have been converted to T_A^* from T_R^* .) The assumed LSR velocity is 19 km s $^{-1}$. The line profiles, which are unusually narrow for this object, suggest a confined source where gas-phase NaCl disappears before the terminal velocity of the outflow is achieved. The features marked “U” are unidentified.

3. RESULTS

Five rotational transitions of NaCl were detected toward VY CMa: four lines at 1 mm measured with the SMT ($J = 17 \rightarrow 16$ through $J = 20 \rightarrow 19$) and an additional transition at 2 mm ($J = 11 \rightarrow 10$) observed at the 12 m telescope. These data are presented in Figure 1. As the figure shows, the intensities are consistent among these five lines detected ($T_A^* \sim 4$ –14 mK), and the LSR velocities are all $V_{\text{LSR}} \sim 18$ km s $^{-1}$ —typical for VY CMa (Ziurys et al. 2007). Furthermore, each transition has a somewhat flat-topped profile, indicating the source of NaCl was not resolved in VY CMa, even with the smallest beam size of $\theta_b \sim 29''$ at the SMT. An unresolved source is also consistent with the observed line widths. As listed in Table 1, typical line widths (FWHM) for NaCl in VY CMa are $\Delta V_{1/2} \sim 15$ km s $^{-1}$, which are considerably smaller than those measured for CO (~ 33 km s $^{-1}$), HCN (~ 33 km s $^{-1}$), and SiO (43 km s $^{-1}$) in this object (Kemper et al. 2003; Ziurys et al. 2007). This finding suggests that NaCl has not yet reached the terminal velocity in VY CMa, estimated to be $V_{\text{exp}} \geq 21$ km s $^{-1}$ (Ziurys et al. 2007; Muller et al. 2007).

Three transitions of NaCl ($J = 18 \rightarrow 17$, $J = 19 \rightarrow 18$, and $J = 20 \rightarrow 19$) were detected toward IK Tau (see Fig. 2); observed line parameters are also listed in Table 1. The spectra show a consistent velocity of $V_{\text{LSR}} \sim 29$ km s $^{-1}$, and intensities near $T_A^* \sim 0.006$ K. As for VY CMa, the line widths of these three transitions are significantly less than those of other known molecular species in this object, with $\Delta V_{1/2} \sim 5$ km s $^{-1}$, as compared to CO and HCN ($\Delta V_{1/2} \sim 23$ km s $^{-1}$; S. N. Milam et al. 2007, in preparation; Nercessian et al. 1989).

In order to obtain a consistent data set for comparison, five transitions of NaCl were additionally measured toward IRC +10216. Line parameters for these spectra are also listed in Table 1.

4. DISCUSSION

4.1. Abundance and Spatial Distribution

The fractional abundance of NaCl, relative to H $_2$ (all fractional abundances are relative to H $_2$), was modeled with a radiative transfer circumstellar code developed by Bieging & Tafalla (1993) for a spherical distribution. Collisional excitation was assumed, using cross sections of SiO, corrected for the mass difference. The dis-

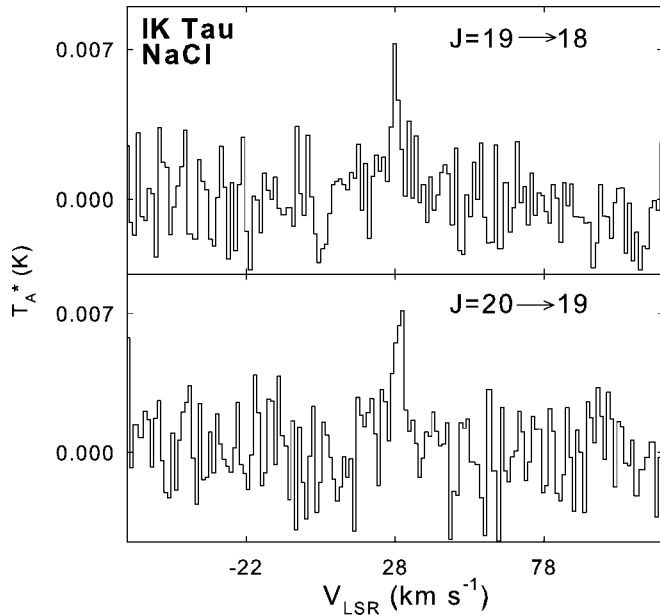


FIG. 2.—The $J = 19 \rightarrow 18$ and $J = 20 \rightarrow 19$ transitions of NaCl in IK Tau, measured with the SMT telescope of the ARO. Spectral resolution is 1 MHz, and the assumed velocity is $V_{\text{LSR}} = 34.5 \text{ km s}^{-1}$. As found in VY CMa, the narrow line widths observed indicate that NaCl does not remain in the gas phase long enough to reach the terminal outflow velocity.

tance to VY CMa was set at 1500 pc with a mass-loss rate of $\sim 10^{-4} M_{\odot} \text{ yr}^{-1}$ and a stellar temperature of $T_{*} \sim 3368 \text{ K}$ (see Ziurys et al. 2007; Humphreys et al. 2007). A mass-loss rate of $4.5 \times 10^{-6} M_{\odot} \text{ yr}^{-1}$, distance of 270 pc, and $T_{*} \sim 2100 \text{ K}$ were assumed for IK Tau (Marvel 2005; Duari et al. 1999). The temperature law used in the modeling was $T \propto r^{-0.7}$, based on other codes written for evolved stars (Kemper et al. 2003; Keady et al. 1988). However, the model results did not significantly change with a constant temperature profile (appropriate only in the inner-shell region) or a $r^{-0.58}$ dependence, as used in other models for the acceleration zone (Justtanont et al. 1994). A r^{-2} dependence was assumed for the density profile, with the initial density derived from a constant mass-loss rate, assuming an expansion velocity of $V_{\text{exp}} \sim 5 \text{ km s}^{-1}$ (VY CMa) or $\sim 3 \text{ km s}^{-1}$ (IK Tau), i.e., half the observed NaCl line width. Calculations were also conducted with an increased density (factor of 5) through the dust acceleration zone, for comparison, to account for additional density enhancements prior to achieving the terminal outflow velocity. This situation was not the case for IRC +10216, where NaCl attained the full expansion velocity, as indicated by the line profiles.

The model was used to reproduce the observed line profiles by varying two parameters: the molecular abundance and source size. For VY CMa, a source size of $0.5''$ with a fractional abundance relative to H_2 of $\sim 5 \times 10^{-9}$ was derived from a fit to all five lines, using the r^{-2} density law (see Table 2). This value is consistent with the size of the dust acceleration zone in VY CMa ($r \sim 0.5''$; Monnier et al. 1999) and the narrow line profiles. However, for IK Tau, the source size could not be constrained by the observational data because the three lines observed were very close in energy. Instead, the source size was estimated from that of the inner dust shell ($d \sim 0.2''$) obtained by Hale et al. (1997), as well as the expansion velocity deduced from the line width. Based on the dynamical model of Bujarrabal et al. (1989), an expansion velocity of $\sim 2.5 \text{ km s}^{-1}$ is achieved in IK Tau at a radius of $5 \times 10^{14} \text{ cm}$, or $\theta_s \sim 0.3''$. A source size of $0.3''$ was therefore assumed, resulting in a fractional abundance relative to H_2 toward

TABLE 2
OBSERVED FRACTIONAL ABUNDANCES OF CIRCUMSTELLAR
SODIUM-BEARING MOLECULES

Molecule	IRC +10216	CRL 2688	VY CMa	IK Tau
NaCl	2.0×10^{-9}	1.6×10^{-10} ^a	5.0×10^{-9}	4.0×10^{-9}
NaCN	2.3×10^{-8} ^a	5.2×10^{-9} ^a	$< 1 \times 10^{-8}$...
NaOH	$< 3 \times 10^{-9}$...
NaF	$< 9 \times 10^{-10}$...

^a From Highberger et al. (2003).

IK Tau of 4×10^{-9} , for the r^{-2} density dependence. For the enhanced density calculations, the fractional abundance in both sources decreased by a factor of ~ 5 . Because the molecular envelopes of VY CMa and IK Tau extend well beyond $10''$ – $20''$, as indicated by HCN and CO observations (Guélin et al. 1996; Nercessian et al. 1989; Ziurys et al. 2007), NaCl is likely incorporated into grains early in the condensation process.

A rotational diagram analysis was also done for comparison. For a source size of $\theta_s \sim 0.5''$, the total column density of $2.4 \times 10^{14} \text{ cm}^{-2}$ was obtained with $T_{\text{rot}} \sim 92 \text{ K}$ for VY CMa, corresponding to a fractional abundance of $f \sim 4 \times 10^{-9}$. This value is in excellent agreement with the model results. This analysis was also conducted for IK Tau, assuming a source size of $\sim 0.3''$. The total column density of NaCl derived was $N_{\text{tot}} = 2.5 \times 10^{14} \text{ cm}^{-2}$ with $T_{\text{rot}} \sim 70 \text{ K}$, or $f \sim 4 \times 10^{-9}$.

4.2. Comparison with Chemical Models

To gain further understanding of refractory abundances, a chemical equilibrium model was used to predict the key Na-bearing species found in the O-rich envelopes (adapted from Tsuji 1973). Figure 3 displays the results of these calculations for a range of temperatures with $\text{C/O} = 0.5$ (solar abundance) and $n \sim 10^{11} \text{ cm}^{-3}$. NaCl is clearly the main carrier of sodium in an oxygen-rich environment for the temperature range 500–1250 K, with $f \sim 10^{-7}$ to 10^{-10} , with NaOH reaching a peak fractional abundance near $T \sim 500 \text{ K}$ at $f \sim 10^{-9}$. NaO, surprisingly, never attains a fractional abundance above $f \sim 10^{-15}$ at any temperature.

Observational results for both oxygen-rich envelopes agree qualitatively with model predictions at $T \sim 1100 \text{ K}$ (see Table 2 for a summary of fractional abundances). This temperature implies formation at a radius of $\sim 5R_{*}$ for VY CMa and $\sim 3R_{*}$ for IK Tau, given the assumed $r^{-0.7}$ dependence and the stellar temperatures of 3368 K (VY CMa) and 2100 K (IK Tau). Presumably, these LTE abundances “freeze out” as the molecules flow from the hotter regions, as predicted by chemical models (McCabe et al. 1979), thus explaining the observed source sizes of $\sim 40R_{*}$ (VY CMa) and $\sim 30R_{*}$ (IK Tau). Rotational temperatures of 70–92 K are consistent with this scenario as well, considering the high dipole moment of NaCl (9.0 D). It should also be noted that NaCN and NaOH were not observed in VY CMa with upper limits of $f \leq 10^{-8}$ (see Table 2). These limits, however, are not sufficiently low to constrain the model.

4.3. Salt in Carbon- versus Oxygen-rich Envelopes

For comparison, the LTE model was also run for the C-rich case ($\text{C/O} = 1.5$) with identical densities and temperatures. As shown in Figure 3, the most noticeable distinction between the two models is the importance of NaCN in carbon-rich gas. This species is at least three orders of magnitude more abundant than in the O-rich case, reaching a peak concentration near 10^{-7} at $T \sim 700 \text{ K}$. The abundance of NaCl roughly follows that of

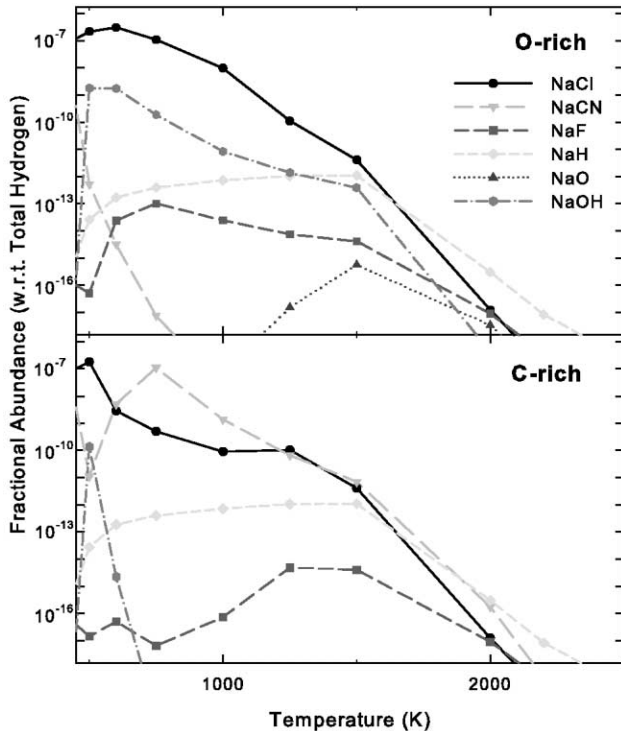


FIG. 3.—Thermodynamic equilibrium calculations of major sodium-bearing species in circumstellar shells that are O-rich (solar composition; *top*) and C-rich ($C/O = 1.5$; *bottom*) at densities $n \sim 10^{11} \text{ cm}^{-3}$ (based on Tsuji 1973). Fractional abundances are plotted with respect to total hydrogen for various temperatures. Abundances determined at $T \sim 1100 \text{ K}$ are in good agreement with the results obtained for VY CMa and IK Tau.

NaCN as a function of temperature, except at 700–1000 K, where NaCN is more abundant than NaCl by about factors of 10–100.

The fractional abundances derived from observations of the C-rich shells IRC +10216 and CRL 2688 are in good agreement with the models (see Table 2). For IRC +10216, the abundances of NaCl and NaCN are well predicted by the model at $T \sim 700 \text{ K}$, with $f(\text{NaCl}) \sim 2 \times 10^{-9}$ and $f(\text{NaCN}) \sim 2 \times$

10^{-8} . For CRL 2688, the best fit is for $T \sim 1000 \text{ K}$. These formation temperatures are consistent with the photosphere temperatures of 2320 and 6600 K for IRC +10216 and CRL 2688. Considering a $r^{-0.7}$ profile, this temperature implies a formation radius of $r \sim 2 \times 10^{14} \text{ cm}$ or $\sim 3R_*$, for IRC +10216. For CRL 2688, the formation radius is much larger ($\sim 11R_*$), although it is unlikely that the temperature profile is so simple in this object. The larger radius, however, is consistent with shock formation induced by the second stage of mass loss, as found by Highberger et al. (2003b).

Despite the chemical differences, NaCl appears to have a distribution close to the star in both oxygen- and carbon-rich envelopes, with a maximum radius of $\sim (6\text{--}10) \times 10^{15} \text{ cm}$, corresponding to $\sim 41R_*$ and $172R_*$ for VY CMa and IRC +10216. In IRC +10216, however, the molecule does reach the terminal velocity of the envelope—not the situation for either VY CMa or IK Tau. The confined distribution of sodium chloride in both types of objects implies that it condenses onto grains. Lodders & Fegley (1999) suggest that NaCl (i.e., crystalline salt) may be a major carrier of sodium in the solid state in C-rich envelopes. These data suggest it could be equally important for O-rich environments, as opposed to sodalite $[\text{Na}_4(\text{AlSi}_3\text{O}_8)_3\text{Cl}]$. The amount of sodium contained in crystalline salt must be controlled by the chlorine abundance, which is $\text{Cl}/\text{H} \sim 3.2 \times 10^{-7}$, as opposed to $\text{Na}/\text{H} \sim 2.1 \times 10^{-6}$, assuming solar composition—an order of magnitude difference. (It should also be noted that sodium may be enriched by hot bottom burning in AGB stars; Izzard et al. 2007.) In O-rich shells, another important condensate for sodium is albite, $\text{NaAlSi}_3\text{O}_8$. This alternative is probably not as prevalent in carbon-rich environments, and may explain why NaCl remains longer in the gas phase for C stars such as IRC +10216.

This research was supported by NSF grant AST 06-07803 and based on work supported by the National Aeronautics and Space Administration through the NASA Astrobiology Institute under cooperative agreement CAN-02-OSS-02 issued through the Office of Space Science. S. N. M. would like to thank the Phoenix Chapter of ARCS, specifically the Mrs. Scott L. Libby, Jr., endowment, for partial funding.

REFERENCES

- Biegging, J. H., & Tafalla, M. 1993, *AJ*, 105, 576
 Bujarrabal, V., Gómez-González, J., & Planesas, P. 1989, *A&A*, 219, 256
 Cernicharo, J., & Guélin, M. 1987, *A&A*, 183, L10
 Duari, D., Cherchneff, I., & Willacy, K. 1999, *A&A*, 341, L47
 Guélin, M., Lucas, R., & Neri, R. 1996, in *CO: Twenty-Five Years of Millimeter Wave Spectroscopy*, ed. W. B. Latter et al. (Dordrecht: Kluwer), 359
 Hale, D. D. S., et al. 1997, *ApJ*, 490, 407
 Highberger, J. L., Thomson, K. J., Young, P. A., Arnett, D., & Ziurys, L. M. 2003, *ApJ*, 593, 393
 Highberger, J. L., & Ziurys, L. M. 2003, *ApJ*, 597, 1065
 Humphreys, R. M., Helton, L. A., & Jones, T. J. 2007, *AJ*, 133, 2716
 Izzard, R. G., Lugaro, M., Karakas, A. I., Iliadis, C., & van Raai, M. 2007, *A&A*, 466, 641
 Justtanont, K., Skinner, C. J., & Tielens, A. G. G. M. 1994, *ApJ*, 435, 852
 Kawaguchi, K., Kagi, E., Hirano, T., Takano, S., & Saito, S. 1993, *ApJ*, 406, L39
 Keady, J. J., Hall, D. N. B., & Ridgway, S. T. 1988, *ApJ*, 326, 832
 Kemper, F., Stark, R., Justtanont, K., de Koter, A., Tielens, A. G. G. M., Waters, L. B. F. M., Cami, J., & Dijkstra, C. 2003, *A&A*, 407, 609
 Lauria, E. F., Kerr, A. R., Reiland, G., Freund, R. F., Lichtenberger, A. W., Ziurys, L. M., Metcalf, M., & Forbes, D. 2006, First Astronomical Observations with an ALMA Band 6 (211–275 GHz) Sideband-Separating SIS Mixer-preamp (ALMA Memo 553), <http://www.alma.nrao.edu/memos>
 Lodders, K., & Fegley, B. 1999, in *IAU Symp. 191, Asymptotic Giant Branch Stars*, ed. T. Le Bertre, A. Lébre, & T. Waelkens (Dordrecht: Kluwer), 279
 Marvel, K. B. 2005, *AJ*, 130, 261
 McCabe, E. M., Connors Smith, R., & Clegg, R. E. S. 1979, *Nature*, 281, 263
 Monnier, J. D., Tuthill, P. G., Lopez, B., Cruzalebes, P., Danchi, W. C., & Haniff, C. A. 1999, *ApJ*, 512, 351
 Muller, S., Dinh-V-Trung, Lim, J., Hirano, N., Muthu, C., & Kwok, S. 2007, *ApJ*, 656, 1109
 Nerecessian, E., Guilloteau, S., Omont, A., & Benayoun, J. J. 1989, *A&A*, 210, 225
 Pardo, J. R., Cernicharo, J., Goicoechea, J. R., Guélin, M., & Asensio Ramos, A. 2007, *ApJ*, 661, 250
 Tsuji, T. 1973, *A&A*, 23, 411
 Turner, B. E., Steimle, T. C., & Meerts, L. 1994, *ApJ*, 426, L97
 Ziurys, L. M., Apponi, A. J., Guélin, M., & Cernicharo, J. 1995, *ApJ*, 445, L47
 Ziurys, L. M., Apponi, A. J., & Phillips, T. G. 1994, *ApJ*, 433, 729
 Ziurys, L. M., Milam, S. N., Apponi, A. J., & Woolf, N. J. 2007, *Nature*, 447, 1094
 Ziurys, L. M., Savage, C., Highberger, J. L., Apponi, A. J., Guélin, M., & Cernicharo, J. 2002, *ApJ*, 564, L45